ISSN 1028-334X, Doklady Earth Sciences, 2016, Vol. 471, Part 1, pp. 1144–1148. © Pleiades Publishing, Ltd., 2016.
Original Russian Text © Yu.V. Bataleva, Yu.N. Palyanov, Yu.M. Borzdov, N.V. Sobolev, 2016, published in Doklady Akademii Nauk, 2016, Vol. 471, No. 1, pp. 77–81.

**GEOCHEMISTRY**

# Graphite and Diamond Formation via the Interaction of Iron Carbide and Fe,Ni-Sulfide under Mantle *P–T* Parameters

**Yu. V. Bataleva[a,b]*, Yu. N. Palyanov[a,b]**, Yu. M. Borzdov[a,b], and Academician N. V. Sobolev[a,b]**

Received June 17, 2016

**Abstract**—Experimental research in the $Fe_3C$–(Fe,Ni)S system was carried out. The objective of the investigation was to model the reactions of carbide–sulfide interaction related to graphite (diamond) formation in reduced lithosphere mantle domains. $T \leq 1200$°C is the formation temperature of the Ni-cohenite + graphite assemblage coexisting with two immiscible melts such as sulfide $(Fe_{60}–Ni_3–S_{37})_L$ and metal–sulfide $(Fe_{71}–Ni_7–S_{21}–C_1)_L$ containing dissolved carbon. $T \geq 1300$°C is the generation temperature of a unified melt such as $(Fe_{80}–Ni_6–S_{10}–C_4)_L$ characterized by graphite crystallization and diamond growth. The extraction of carbide carbon during the interaction with the sulfide melt can be considered as one of the potential mechanisms of graphite and diamond formation in the reduced mantle.

**DOI:** 10.1134/S1028334X16110015

According to recent ideas, carbon (C) is one of the most common volatile components in the Earth's mantle. Its average concentrations in mantle rocks reach 80–400 ppm [1, 2]. Due to the fact that C is an element with a variable valency, the form in which it occurs in the mantle is primarily dependent on the oxygen ($O_2$) fugacity values. In relatively oxidized mantle domains, C can occur in carbonates, $CO_2$ fluid, or carbonate-bearing melts [1, 2]. In the reduced lithospheric mantle, the most likely C concentrators include diamond, graphite, carbide, or Fe,Ni-metallic phases containing dissolved C [1–5]. The assemblage of carbon-containing phases is dependent on the gross concentrations of C in the mantle rocks. In particular, it is assumed that total C is dissolved in metal in the depleted mantle (about 20–120 ppm C), and it occurs in carbides ($Fe_3C$, $Fe_7C_3$), diamond, and graphite in the nondepleted mantle (up to 800 ppm C) [1, 5].

One of the topical issues discussed concerning the problem of global carbon cycle and diamond genesis [4] and requiring primarily an experimental solution is the source of C in diamond crystallization in reduced lithospheric mantle conditions. Some researchers suggest that iron carbide may play the role of the C source in diamond formation processes under reducing conditions [1, 4, 5]. The potential genetic relation of diamond and carbide is confirmed by cohenite findings in inclusions of natural diamonds [6, 7]. However, according to most works related to modeling of natural diamond-forming environments, graphite is considered to be the C source, while experimental data on diamond crystallization from the carbon of carbonate and carbide are still insufficient [8, 9].

According to the results of our experimental investigations, C can be extracted from Fe carbide under its interaction with S-enriched fluid, which is a common metasomatic agent in the Earth's depths [1, 10]. The $Fe_3C$ interaction with an Fe,Ni-sulfide melt can be considered as one of the potential scenarios of elementary C formation from Fe carbide. The occurrence of an Fe,Ni-sulfide melt in the diamond crystallization environment is confirmed by numerous findings of sulfides as inclusions in diamonds and minerals of diamondiferous mantle xenoliths [6]. The objective of our investigation is to estimate the possibility of potential elementary C formation as a result of the interaction between carbide and Fe,Ni-sulfide under the reduced mantle conditions, to study the generation conditions and composition of carbon-forming melts, and to assess the effect of Ni impurity on the stability of Fe carbide in the presence of sulfides or a sulfide melt.

The experimental studies in the carbide–sulfide system were carried out using the multi-anvil high-pressure apparatus of a "split-sphere" type at 6.3 GPa, 1100–1500°C, and 20 h. The initial reagents included Fe carbide (cohenite) presynthesized at 6 GPa and 1300°C and synthetic Ni-pyrrhotite ($Fe_{0.7}Ni_{0.3}S$). The mass proportions of cohenite and Ni-pyrrhotite reached 3 : 1. Ground (up to 20–50 μm) and thor-

---

[a] *Sobolev Institute of Geology and Mineralogy, Siberian Branch, Russian Academy of Sciences, pr. Akad. Koptyuga 3, Novosibirsk, 630090 Russia*
[b] *Novosibirsk State University, Novosibirsk, 630090 Russia*
*e-mail: *bataleva@igm.nsc.ru, **palyanov@igm.nsc.ru*

**Table 1.** Experimental data on carbide–sulfide interaction in the $Fe_3C$–(Fe,Ni)S system at 6.3 GPa, 1100–1500°C over 20 h

| Exp. no. | T, °C | Final phases | Mass portions of final phases, wt %* | | | | |
|---|---|---|---|---|---|---|---|
| | | | Coh | $L_1$ | $L_2$ | $L_3$ | Gr |
| 982/7 | 1100 | Coh, Gr, $L_1$, $L_2$ | 56 | 15 | 28 | – | 1 |
| 983/7 | 1200 | Coh, Gr, $L_1$, $L_2$ | 50 | 6 | 43 | – | 1 |
| 984/7 | 1300 | $L_3$, Gr | – | – | – | 99 | 1 |
| 981/7 | 1400 | $L_3$, Gr | – | – | – | 98 | 2 |
| 985/7 | 1500 | $L_3$, Gr | – | – | – | 98 | 2 |

Here and in Table 2: (Coh) cohenite, ($L_1$) sulfide melt, ($L_2$, $L_3$) metal–sulfide melts with dissolved C, (*) calculation is carried out by the mass balance method.

oughly mixed initial reagents were placed in graphite ampoules in the course of assembly. Seed cube octahedral diamond crystals (500 μm) were put in the reaction volume of the ampoules. The selection of graphite as the optimum material of ampoules was related to experience working with sulfides and S under mantle P, T [9–11]. After the experiments, the samples were subjected to rapid quenching (150–200°C/s) to study in detail the specific features of the compositions of melts formed in the reaction volume. The bulk composition of the quenching aggregates obtained adequately reflected the compositions of the melts occurring in the samples under the experimental P–T parameters.

The phase and chemical compositions of the samples were determined by microprobe analysis and energy dispersive spectroscopy (Tescan MIRA3 LMU scanning electron microscope). Carbide phases were shot at an accelerating voltage of 20 kV, probe current of 20 nA, account time of 10 s in each analytical line, and electron beam probe diameter of 2–4 μm. The electron beam diameter was increased to 20–60 μm in the investigation of the compositions of quenched sulfide and metal–sulfide melts with dissolved carbon, which are microdendrite aggregates. The phase relations in the samples were studied by scanning electron microscopy. The analytical studies were carried out at the Center for Collective Use of Multielement and Isotopic Studies, Siberian Branch, Russian Academy of Sciences. The mass proportions of the obtained phases were calculated by the mass balance method.

The experimental results and compositions of the phases obtained are given in Tables 1 and 2. At lower temperatures (1100, 1200°C), the samples were identified to have large (over 1 mm) elongated $Fe_{2.95}Ni_{0.05}C$ carbide crystals with a quenching pyrrhotite + taenite aggregate (Fig. 1a) and graphite crystals (20–30 μm) in the intergranular space. These data are indicative of the fact that basic processes under the given P and T involve sulfide melting, cohenite recrystallization, and carbon-forming reactions resulting in graphite crystallization. As follows from the analysis of quenching aggregates, at $T \geq 1100°C$ the carbide–sulfide interaction is accompanied by the generation of two immiscible melts such as the sulfide melt $(Fe–Ni–S)_L$ and metal–sulfide with dissolved carbon $(Fe–Ni–S–C)_L$ (Fig. 1a). These melts are characterized by the following bulk compositions: ~$Fe_{60}$–$Ni_3$–$S_{37}$ and ~$Fe_{71}$–$Ni_7$–$S_{21}$–$C_1$, respectively (from here on, the melt compositions are given in wt %) (Table 2). The basic reaction, which is characterized by carbide–sulfide interaction at 1100–1200°C, is as follows (schematic form):

$$\begin{aligned} &Fe_3C + Fe_{0.7}Ni_{0.3}S \rightarrow (Fe,Ni)_3C \\ &+ (Fe–Ni–S)_L + (Fe–Ni–S–C)_L + C^0_{(graphite)}. \end{aligned} \quad (1)$$

At 1300–1500°C cohenite is absent in the experimental products, while the samples occur as coarse-crystalline graphite (70–250 μm) (Fig. 1b) and a homogeneous quenching aggregate of the $(Fe–Ni–S–C)_L$ melt, which is composed of microdendritic carbide, taenite, and pyrrhotite (Fig. 1c). Diamond grows on the (111) and (100) facets in crystal seeds (Fig. 1d). The bulk composition of the metal–sulfide melt with dissolved C depending on temperature varies from ~$Fe_{76}Ni_6S_{13}C_5$ (1300°C) to ~$Fe_{80}Ni_6S_{10}C_4$ (1500°C). At 1300–1500°C the interaction in the system corresponds to the following schematic reaction:

$$\begin{aligned} &Fe_3C + Fe_{0.7}Ni_{0.3}S \\ &\rightarrow (Fe–Ni–S–C)_L + C^0_{(graphite,diamond)}. \end{aligned} \quad (2)$$

The potential graphite crystallization mechanism in reaction (1) was determined by reconstruction of the carbide–sulfide interaction at relative low temperatures ($T \leq 1200°C$). The Fe carbide interaction with the Fe,Ni-sulfide melt is accompanied by cohenite recrystallization, Fe extraction into the sulfide melt, and enrichment of recrystallized cohenite in nickel. C released from carbide is largely crystallized as graphite. Graphite is established to be crystallized

**Table 2.** Average phase compositions obtained as a result of carbide–sulfide interaction based on microprobe analysis data

| Exp. no. | $T$, °C | Phase | Composition, wt % | | | | | Composition, at % | | | |
|---|---|---|---|---|---|---|---|---|---|---|---|
| | | | Fe | Ni | S | C | total | Fe | Ni | S | C |
| 982/7 | 1100 | $L_1$ | $60.7_{(5)}$ | $2.6_{(1)}$ | $36.4_{(4)}$ | – | $99.8_{(8)}$ | $47.8_{(2)}$ | $2.0_{(0)}$ | $50.2_{(0)}$ | – |
| | | $L_2$ | $71.0_{(4)}$ | $7.2_{(5)}$ | $20.5_{(4)}$ | $1.2_{(0)}$ | $100.0_{(5)}$ | $59.4_{(6)}$ | $5.8_{(1)}$ | $30.0_{(0)}$ | $4.8_{(0)}$ |
| | | Coh | $92.3_{(1)}$ | $1.0_{(1)}$ | – | $6.7_{(1)}$ | $100.0_{(1)}$ | $74.2_{(0)}$ | $0.8_{(2)}$ | – | $25.0_{(2)}$ |
| 983/7 | 1200 | $L_1$ | $60.6_{(2)}$ | $2.3_{(0)}$ | $36.5_{(6)}$ | – | $99.5_{(4)}$ | $47.8_{(5)}$ | $1.8_{(0)}$ | $50.4_{(0)}$ | – |
| | | $L_2$ | $72.1_{(5)}$ | $5.1_{(2)}$ | $21.0_{(6)}$ | $1.8_{(4)}$ | $100.0_{(0)}$ | $59.1_{(2)}$ | $4.0_{(1)}$ | $30.1_{(0)}$ | $6.8_{(11)}$ |
| | | Coh | $92.0_{(1)}$ | $1.3_{(1)}$ | – | $6.7_{(1)}$ | $100.0_{(1)}$ | $74.0_{(1)}$ | $1.0_{(2)}$ | – | $25.0_{(2)}$ |
| 984/7 | 1300 | $L_3$ | $76.6_{(7)}$ | $6.1_{(4)}$ | $13.0_{(6)}$ | $4.4_{(6)}$ | $100.0_{(0)}$ | $61.0_{(1)}$ | $4.6_{(2)}$ | $18.0_{(0)}$ | $16.3_{(6)}$ |
| 981/7 | 1400 | $L_3$ | $79.4_{(8)}$ | $6.2_{(3)}$ | $10.8_{(7)}$ | $3.6_{(3)}$ | $100.0_{(0)}$ | $65.7_{(11)}$ | $4.9_{(2)}$ | $15.6_{(0)}$ | $13.8_{(5)}$ |
| 985/7 | 1500 | $L_3$ | $80.5_{(11)}$ | $5.5_{(6)}$ | $10.1_{(9)}$ | $3.9_{(9)}$ | $100.0_{(0)}$ | $66.3_{(3)}$ | $4.3_{(2)}$ | $14.5_{(1)}$ | $14.8_{(7)}$ |

Standard deviation values 1σ, in particular for the last sign, are shown in parentheses. $60.7_{(5)}$ means 60.7 ± 0.5.

**Table 3.** Minimum formation parameters of graphite and diamond in the Fe–Ni–S–C-based systems at 5.5–7 GPa (published data)

| System composition (wt %) | Initial reagents | $P$, GPa | $T$, °C | $t$, h | C phases | | | Source |
|---|---|---|---|---|---|---|---|---|
| | | | | | Gr | DG | DN | |
| $Fe_{81}$–$Ni_5$–$S_9$–$C_5$ | Coh, Ni–Po | 6.3 | 1100–1300 | 20 | + | – | – | This work |
| | ″ | 6.3 | 1400–1500 | 20 | + | + | – | ″ |
| $Fe_{34}$–$Ni_{54}$–$S_9$–$C_3$ | Fe–Ni melt, $S^0$, Gr | 6.0 | 1100–1200 | 55 | + | – | – | [11] |
| $Fe_{32}$–$Ni_{52}$–$S_{13}$–$C_3$ | Fe–Ni melt, $S^0$, Gr | 6.0 | 1100 | 55 | + | – | – | ″ |
| $Fe_{32}$–$Ni_{33}$–$S_{33}$–(C) | Pn, Gr | 6.3 | 1450 | 65 | + | + | – | [10] |
| | ″ | 7.0 | 1550–1800 | 20–46 | + | + | – | ″ |
| | ″ | 7.0 | >1800 | 15–40 | + | + | + | ″ |

(Gr) graphite, (DG) diamond growth on crystal seeds, (DN) spontaneous diamond nucleation, (C) graphite ampoule, (Ni–Po) Ni-containing pyrrhotite, and (Pn) pentlandite.

directly in the $(Fe_{71}$–$Ni_7$–$S_{21}$–$C_1)_L$ melt, while Fe,Ni-carbide is a C source. At 1300–1500°C the $Fe_{76-80}Ni_6S_{10-13}C_{4-5}$ melt is an environment of graphite crystallization and diamond growth. Table 3 provides the available published data on the $P$–$T$ parameters of graphite formation and diamond nucleation and growth depending on the Fe–Ni–S–C system composition [11, 12]. The specific features found in graphite crystallization from a largely metal melt that contains dissolved C and S are in good agreement with the investigation results obtained for systems with up to 7–13 wt % S [12] and confirm the ideas of the fact that S is an inhibitor of diamond and graphite generation from metal–carbon melts [13].

Comparison of the data obtained with the results of recent experimental works carried out in the Fe–C–S [9, 14], Fe–Ni–C [4], and Fe–Ni–S–C systems [11–13] under mantle $P$ and $T$ makes it possible to expand the current ideas of regularities in phase formation in the Fe–Ni–S–C system at a relatively low Ni content (5 wt %), because all previous experimental studies in this system were carried out at 33–54 wt % Ni (Table 3). Cohenite stability in the presence of the metal–sulfide melt in the Fe–Ni–S–C system is related to the S concentration and is just slightly dependent on Ni/(Ni + Fe). Meanwhile, the Ni concentration directly affects the immiscibility parameters of the melts obtained. It is known that the Fe–C–S system is characterized by the coexistence of two melts (S-rich melt and Fe,C-rich melt) in a wide temperature range under mantle pressure [14], while almost no such data on the Fe–Ni–S–C system are available. According to [15], the coexistence of two melts such as $(Fe$–$Ni$–$S)_L$ and $(Fe$–$Ni$–$S$–$C)_L$ in the more complicated Fe–Ni–S–

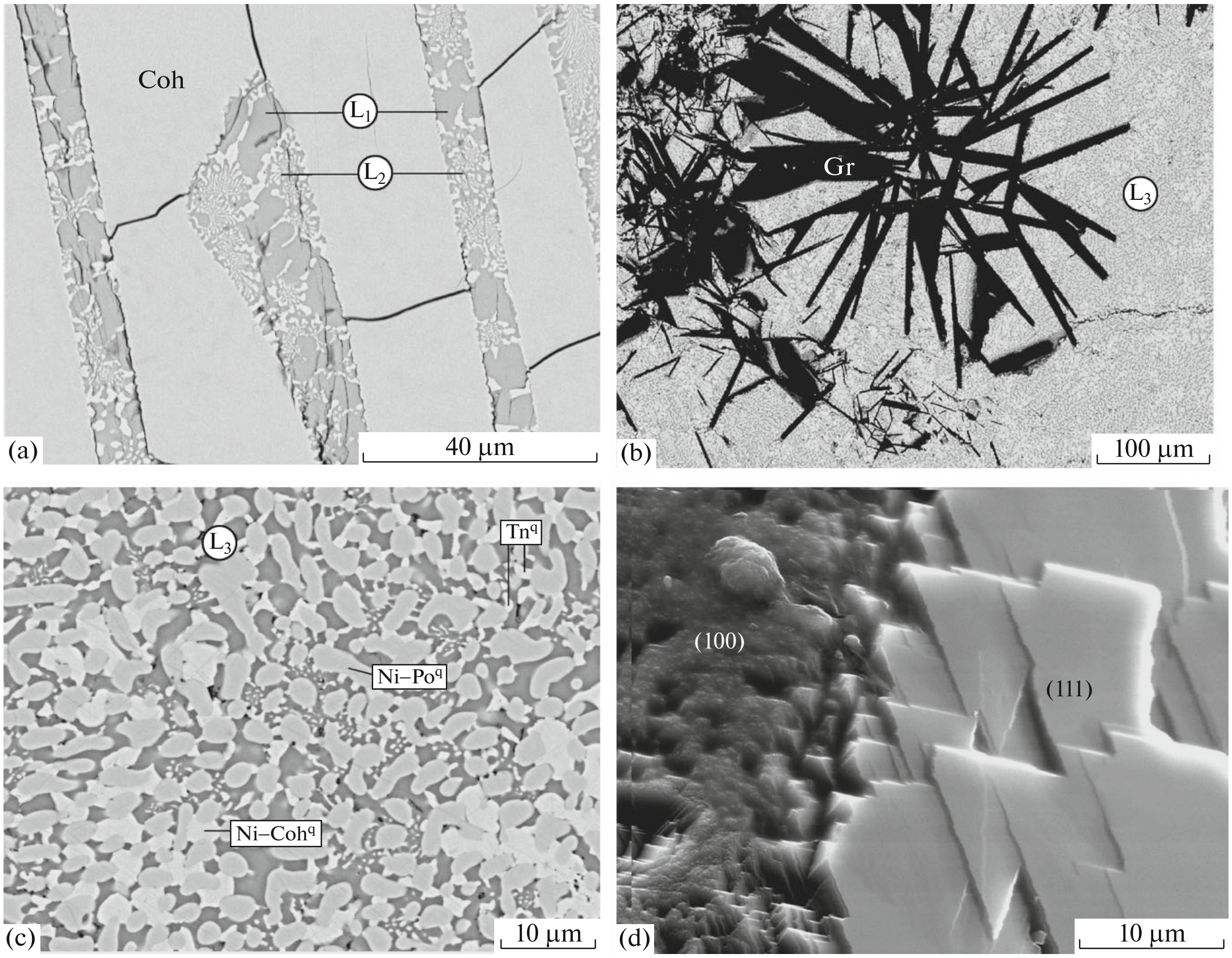

**Fig. 1.** REM microimages: (a) cohenite crystals in the quenching aggregate (1100°C); (b) graphite crystals in the quenching aggregate (1400°C); (c) quenching aggregate structure (1400°C); (d) micromorphology of the (111) and (100) facets in the diamond crystal seed (1400°C); (Coh) cohenite, (Gr) graphite, (Tn) taenite, (Ni–Po) Ni-pyrrhotite, (Ni–Coh) Ni-cohenite, (q) quenching phase, ($L_1$) sulfide melt, ($L_2$, $L_3$) metal–sulfide melts with dissolved C.

C–O system, which models chondrite compositions, is possible only at 1750–2000°C, 5 GPa. As follows from the results of our investigation, two immiscible melts are formed at $T \leq 1200$°C, 6.3 GPa in the $Fe_{81}$–$Ni_5$–$S_9$–$C_5$ system, while a unified melt is generated at higher temperatures.

Hence, the carbide interaction with Fe,Ni-sulfide (or sulfide melt) can be one of the potential C-generating processes under the reduced mantle conditions. According to the experimental results, basic processes of the Fe carbide interaction with the Fe,Ni-sulfide melt, which result in graphite formation and diamond growth, include carbide recrystallization in the sulfide melt, C and Fe extraction from carbide, and formation of a largely metal–sulfide melt with dissolved C (~$Fe_{76-80}Ni_6S_{10-13}C_{4-5}$). As follows from the results obtained, C extraction from Fe carbide during interaction with the sulfide melt can be regarded as one of the potential mechanisms of graphite and diamond formation in the reduced mantle.

## ACKNOWLEDGMENTS

This work was supported by the Russian Foundation for Basic Research, project no. 16-35-60024. This investigation was carried out under a state assignment (project no. VIII.67.3.1).

## REFERENCES

1. R. W. Luth, in *Reference Module in Earth Systems and Environmental Sciences. Treatise on Geochemistry* (Elsevier, Oxford, 2014), pp. 355–391.
2. S. B. Shirey, P. Cartigny, D. G. Frost, et al., Rev. Mineral. Geochem. **75**, 355–421 (2013).
3. A. Rohrbach, C. Ballhaus, U. Golla-Schindler, et al., Nature **449** (7161), 456–458 (2007).

4. A. Rohrbach, S. Ghosh, M. W. Schmidt, et al., Earth Planet. Sci. Lett. **388**, 211–221 (2014).
5. D. J. Frost and C. A. McCammon, Annu. Rev. Earth Planet. Sci. **36**, 389–420 (2008).
6. G. Bulanova, J. Geochem. Explor. **53**, 1–23 (1995).
7. D. E. Jacob, A. Kronz, and K. S. Viljoen, Contrib. Mineral. Petrol. **146** (5), 566–576 (2004).
8. Y. N. Palyanov, Y. V. Bataleva, Y. M. Borzdov, et al., Proc. Nat. Acad. Sci. U.S.A. **110** (51), 20408–20413 (2013).
9. Yu. V. Bataleva, Yu. N. Palyanov, Yu. M. Borzdov, et al., Dokl. Earth Sci. **463** (1), 707–711 (2015).
10. Y. V. Bataleva, Y. N. Palyanov, Y. M. Borzdov, et al., Geology **44** (4), 271–274 (2016).
11. Yu. N. Palyanov, Yu. M. Borzdov, A. F. Khokhryakov, et al., Earth Planet. Sci. Lett. **250**, 269–280 (2006).
12. K. Tsuno and R. Dasgupta, Earth Planet. Sci. Lett. **412**, 132–142 (2015).
13. A. I. Chepurov, Geol. Geofiz., No. 8, 119–124 (1988).
14. L. Deng, Y. Fei, X. Liu, et al., Geochim. Cosmochim. Acta **114**, 220–233 (2013).
15. A. Corgne, B. J. Wood, and Y. Fei, Geochim. Cosmochim. Acta **72**, 2409–2416 (2008).

*Translated by E. Maslennikova*